

TURNING MACHINABILITY OF SHORT POTASSIUM TITANATE FIBER REINFORCED ALUMINUM ALLOY COMPOSITES

K. Asano^{1*}, H. Yoneda¹ and K. Higashi²

¹Department of Mechanical Engineering, School of Science and Engineering, Kinki University, 3-4-1 Kowakae Higashiosaka 577-8502, Japan

²Material R&D Department, Kubota Corporation, 1-1-1 Hama Amagasaki 661-8567, Japan

*asano@mech.kindai.ac.jp

Keywords : aluminum matrix composite, potassium titanate fiber, squeeze casting, machinability

Abstract

Aluminum alloy composites reinforced with short potassium titanate fibers were fabricated by squeeze casting, and the effect of the fiber reinforcement on the turning machinability of the aluminum alloy were investigated. The cutting force and the roughness of the machined surface were reduced by the reinforcement. Short-serrated chips were formed after cutting the composites, while continuous chips were formed after cutting the unreinforced aluminum alloy. Tool wear after cutting has also been investigated.

1 Introduction

The use of aluminum alloys has increased in many industrial applications because the reduction in the weight and size of the products, such as automobile parts, has recently been promoted. These applications often require an improvement in the strength, rigidity, heat resistance and wear resistance of the aluminum alloy. To satisfy these requirements, the reinforcement of the aluminum alloy with ceramic fibers or particles has been proposed. The aluminum alloy composites reinforced with the ceramic fibers or particles have been not only fundamentally evaluated, but also made by way of trials or put into practical use [1]. However, there is a concern about a decrease in the machinability of the aluminum alloy by reinforcing with ceramics, because ceramics are generally difficult to machine. Therefore, it is very important to clarify the machinability of these composites. To develop a machinable aluminum alloy composite having a low thermal expansion rate, we have focused on potassium titanate as the reinforcement because it has a low thermal expansion and hardness. Although several investigations have been conducted on the aluminum alloy composites reinforced with potassium titanate whiskers [2-6], the whiskers are considered harmful to the respiratory organs [7]. The short potassium titanate fiber, having a greater diameter and length than the whisker, was developed to reduce this concern [8]. Based on these findings, we fabricated aluminum alloy composites reinforced with the short potassium titanate fibers by squeeze casting, and clarified that the thermal expansion coefficient of the composite was lower than that of the unreinforced aluminum alloy [9].

In the present study, short potassium titanate fiber reinforced aluminum alloy composites

were fabricated, and the effects of the fiber in the composite and cutting conditions on the machinability were clarified by measuring the cutting resistance, tool wear and roughness of the machined surface and observing the chip forms.

2 Experimental Procedure

The JIS (Japanese Industrial Standards) -AC8A aluminum alloy with its chemical composition shown in Table 1 was used as the matrix metal. Two kinds of short potassium titanate fibers (TXAX, Kubota Co.), which have a different size and hardness, were used as the reinforcements (hereinafter denoted as fibers A and B). Potassium titanate whiskers and aluminum borate whiskers were also used to compare the machinability of the composites with the composites reinforced with fibers A and B. The composition and properties of the reinforcements [6, 8] are shown in Table 2. The Vickers hardness of the fibers is 250-300HV, which is considerably lower than that of the aluminum borate whisker and alumina (1500-2000 HV [10]). Figure 1 is SEM micrographs of the reinforcements.

Si	Mg	Mn	Fe	Cu	Ni	Al
11.8	0.95	0.01	0.08	0.99	1.05	Bal.

Table 1. Chemical composition of aluminum alloy [mass%].

	Short potassium titanate fiber A	Short potassium titanate fiber B	Potassium titanate whisker (TW)	Aluminum borate whisker (BW)
Composition	$K_2Ti_6O_{13}$		$K_2Ti_8O_{17}$	$9Al_2O_3 \cdot 2B_2O_3$
Melting point [K]	1583		1573	1693
Average length [μm]	65	45	15	20
Average diameter [μm]	13	10	0.5	1.0
Hardness [HV]	250	300	350	1000

Table 2. Properties of reinforcements [6,8].

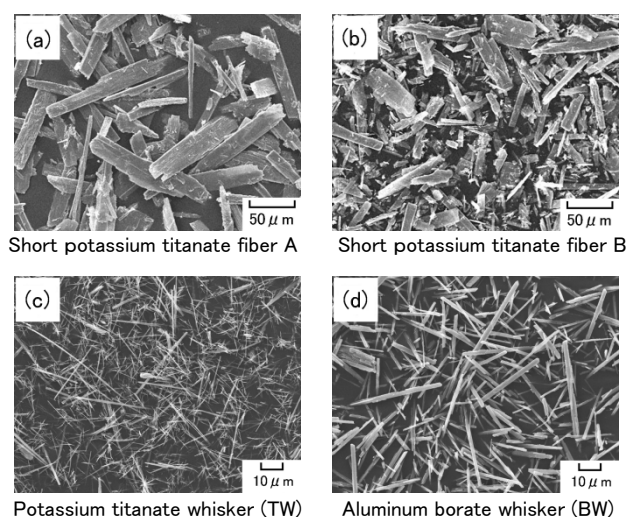


Figure 1. SEM micrographs of reinforcements.

The preforms were fabricated as follows. The reinforcements were dispersed using careful agitation in an aqueous medium containing polyvinyl alcohol (PVA) as the organic binder and

Al₂O₃ sol as the inorganic binder. Dewatering was conducted by press forming, followed by drying at 373 K for 3 hours to drive off any residual free water and to obtain the strength due to the PVA. After drying, the preform was sintered at 1173 K for 1 hour to burn off the PVA and generate the strength due to the presence of the Al₂O₃ binder. The preform had a 50 mm diameter and 20 mm thickness. The preforms contained 25 and 45 vol% of the reinforcement, respectively. In the preform, the reinforcements were oriented in a random configuration.

The composite was fabricated by squeeze casting. The preform was horizontally placed in the permanent mold, and the aluminum alloy melt (1073 K) was poured into the mold (673 K). Pressure (40 MPa) was quickly applied and maintained until the solidification was complete.

The test piece with a 40 mm diameter was machined from the composite, clamped in a lathe, and then the machinability was examined by cutting the outside surface of the test piece with a cemented carbide cutting tool. The cutting conditions are shown in Table 3. The cutting resistances (cutting force) were measured with an elastic disc-type tool dynamometer, and roughness of the machined surface was measured with a surface profiler. The machined surface, cross section and chip forms of the specimens were observed. The width of the flank wear of the tool was measured by observing the flank of the tools after cutting the composite with a numerically-controlled lathe. Taking the practical finishing cut into consideration, the tool wear was measured for the cutting depth of 0.1 mm.

Cutting tool	Carbide (H1)
Rake angle	5°
End cutting edge angle	15°
Nose radius (mm)	0.8
Cutting speed (m/min)	50, 100, 150
Cutting depth (mm)	1.0
Feed rate (mm/rev)	0.10, 0.20
Cutting fluid	None

Table 3. Cutting conditions.

3 Results and Discussion

3.1 Microstructure and hardness of composites

The macrostructure of the vertical cross-section of the composites indicated that the melt infiltration was perfectly accomplished with no observable defects. The height of the composite was approximately 20 mm, which is almost equal to that of the preform before the infiltration. This indicates that the infiltration was successful without any preform contraction or deformation.

Figure 2 is the optical micrographs of the parallel section of the composites. The reinforcements were observed as the dark phases in the micrographs. No agglomeration of the reinforcements or porosity is observed in the composite, indicating that the melt infiltration into the preform was perfectly accomplished. The reinforcements were in a random arrangement.

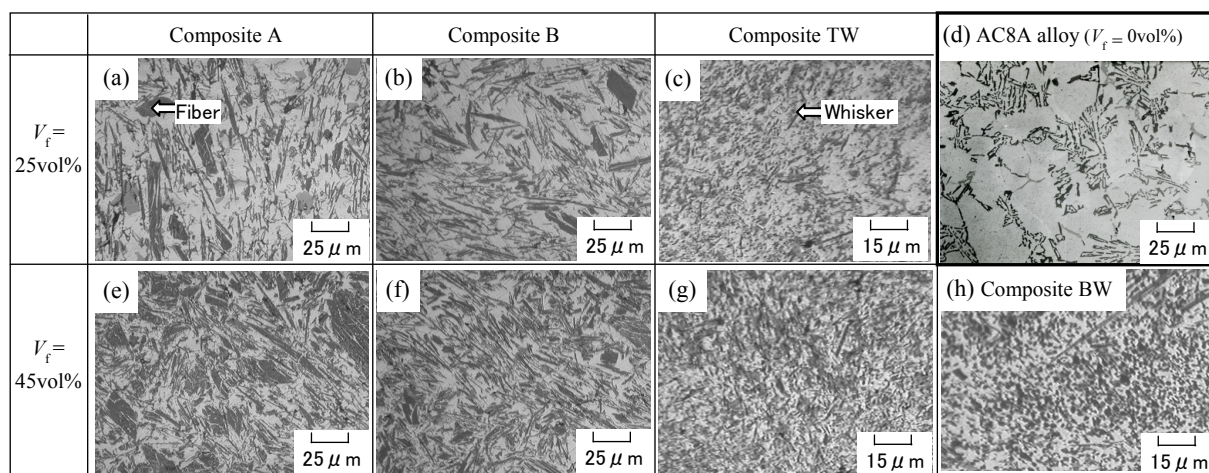


Figure 2. Microstructure in parallel section of composites. V_f represents the fiber volume fraction in composite.

Composite V_f (vol%)	A	B	TW	BW
25	123	147	170	-
45	191	192	208	292

Hardness of AC8A alloy is 90 HV. Composite BW with 25 vol% whisker was not fabricated.

Table 4. Hardness of composites [HV].

Table 4 shows the Vickers hardness of the composites. It shows that the hardness increased as the fiber volume fraction (hereinafter V_f) increased. The hardness of composite BW was the highest due to the highest hardness of the reinforcement.

3.2 Machinability of composites

Figure 3 shows the effect of V_f , the feed rate f , and the cutting speed v on the cutting force F_c of the AC8A (unreinforced) alloy and composites. At every cutting speed and feed rate, F_c of the composites were lower than that of AC8A alloy; reinforcement with the fiber or whisker decreased the F_c . Furthermore, the F_c of composites A and B were lower than those of whisker-reinforced composites (composites TW and BW). It is considered that the reinforcement in the composite has opposite roles; the role to facilitate the shear deformation by generating a high stress concentration as an inclusion and the role as an inclusion to inhibit the shear deformation [11]. The decrease in F_c by the reinforcement is probably due to the former role; the existence of the fibers or whiskers facilitates the shear deformation of the chips during the cutting. It should be noted, however, that the F_c of the composites with a 45 vol% reinforcement is similar to that of the composites with a 25 vol% reinforcement. This is probably due to the offset of the former and the latter roles. At every cutting speed, the F_c increased as f increased. This is due to the increase in the cutting area by increasing the feed rate. The F_c of every specimen little changed even if v increased.

Figure 4 shows the effect of V_f and feed rate f on the surface roughness (maximum height) R_z of the AC8A alloy and composites ($v = 150$ m/min). For every cutting condition, the R_z values of the composites were considerably lower than those of the AC8A alloy. The R_z values of the fiber-reinforced composites (composites A and B) were slightly higher than those of the

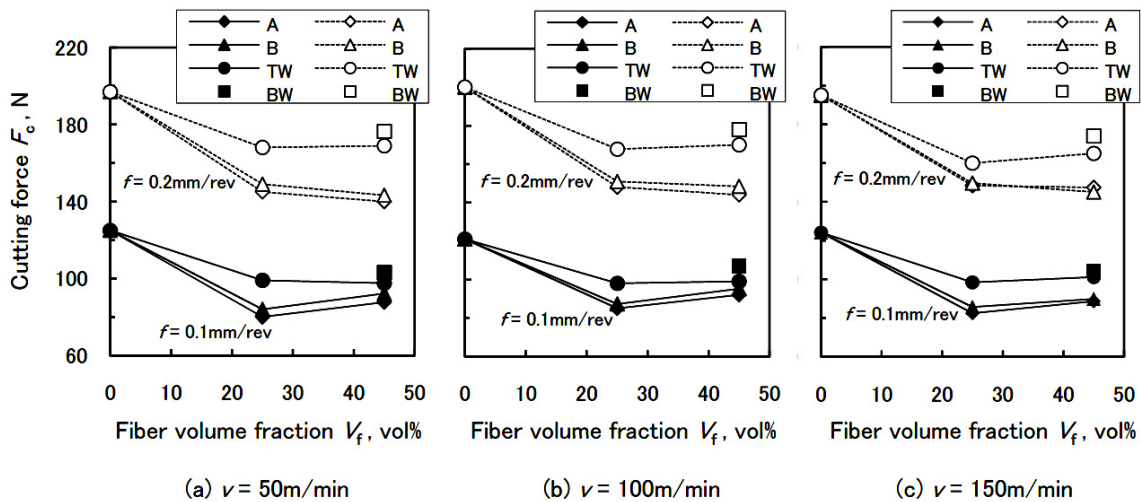


Figure 3. Effect of fiber volume fraction V_f , feed rate f , and cutting speed v on cutting force F_c of AC8A alloy and composites.

whisker-reinforced composites (composites TW and BW). A comparison between Figs. 4(a) and (b) shows that R_z increased as f increased for every specimen. The theoretical roughness can be geometrically obtained from the nose radius of the cutting tool and feed rate [12]. It can be written as

$$R_{th} = \frac{f^2}{8r} \quad (1)$$

where R_{th} is the theoretical roughness and r is the nose radius. The values of R_{th} calculated using eq.(1) are shown in Fig. 4 with the experimental values. Generally, the surface roughness value is higher than R_{th} because the formation of the built-up edge and the accretions formed on the rake face of the tool roughen the machined surface [12]. Figure 4 suggests that it is noticeable for the AC8A alloy ($V_f = 0$ vol%). Under every cutting condition, the R_z values approached the R_{th} values due to the reinforcement. The decrease in R_z by the reinforcement shown in the present study is probably due to the fact that the fibers or whiskers suppressed the formation of the built-up edge and the accretions on the rake face.

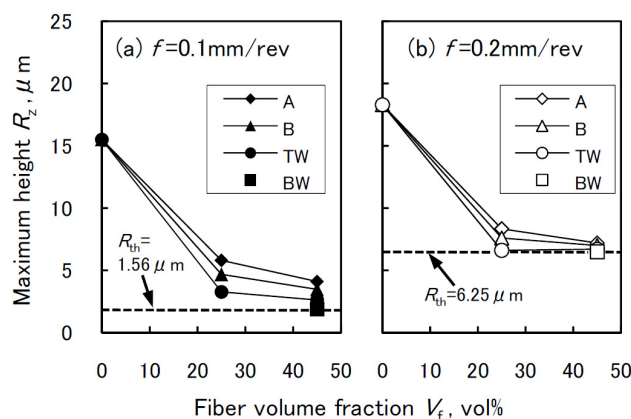


Figure 4. Effect of fiber volume fraction V_f , feed rate f on surface roughness R_z of AC8A alloy and composites at the cutting speed of 150 m/min. R_{th} represents the theoretical roughness.

Figure 5 is SEM micrographs of the machined surfaces of the AC8A alloy and composites with 45 vol% reinforcements ($v = 50$ m/min, $f = 0.2$ mm/rev). On the machined surfaces of the

AC8A alloy (Fig. 5(a)), plastic flow is pronounced. In contrast, the machined surfaces of the composites (Fig. 5(b)-(d)) are smoother than that of the AC8A alloy. An enlarged view of the machined surface of composite A is shown in Fig. 6. The surface is smooth, indicating that the fibers facilitated the shear deformation during the cutting.

Figure 7 shows the chip forms of the AC8A alloy and composites ($v = 100$ m/min, $f = 0.1$ mm/rev). Continuous chips were formed after cutting the AC8A alloy (Fig. 7(d)), while sheared or serrated chips were formed after cutting the composites. In addition, the chips were shorter when V_f was high.

The tendencies observed in Figs. 4-7 were also observed at every cutting speed and feed rate. It is reported that dispersing the hard phases in the aluminum alloy facilitates the shear deformation of the alloy due to the stress concentration in the hard phase during the cutting [11, 13]. The results that occurred in the present study can be expressed by the same mechanism; the fibers in the composite facilitate the shear deformation and division of the chips because the fibers are easily sheared by the cutting.

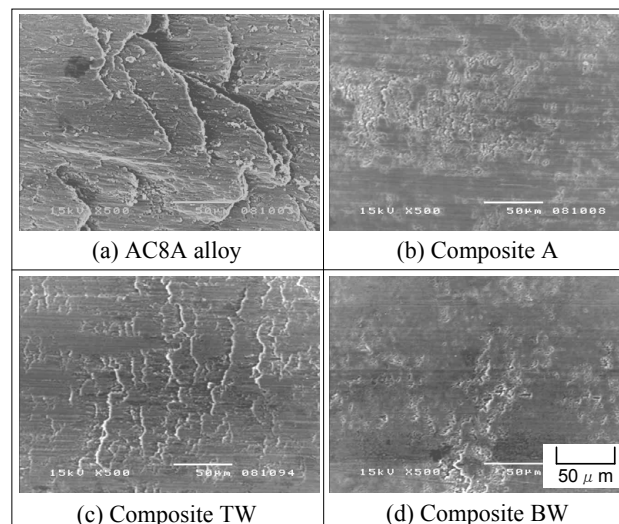


Figure 5. SEM micrographs of machined surfaces of AC8A alloy and composites ($V_f = 45$ vol%) ($v = 50$ m/min, $f = 0.2$ mm/rev).

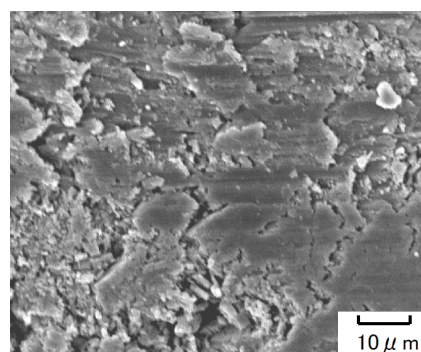


Figure 6. Enlarged view of machined surface of composite A ($V_f = 45$ vol% , $v = 50$ m/min, $f = 0.2$ mm/rev).

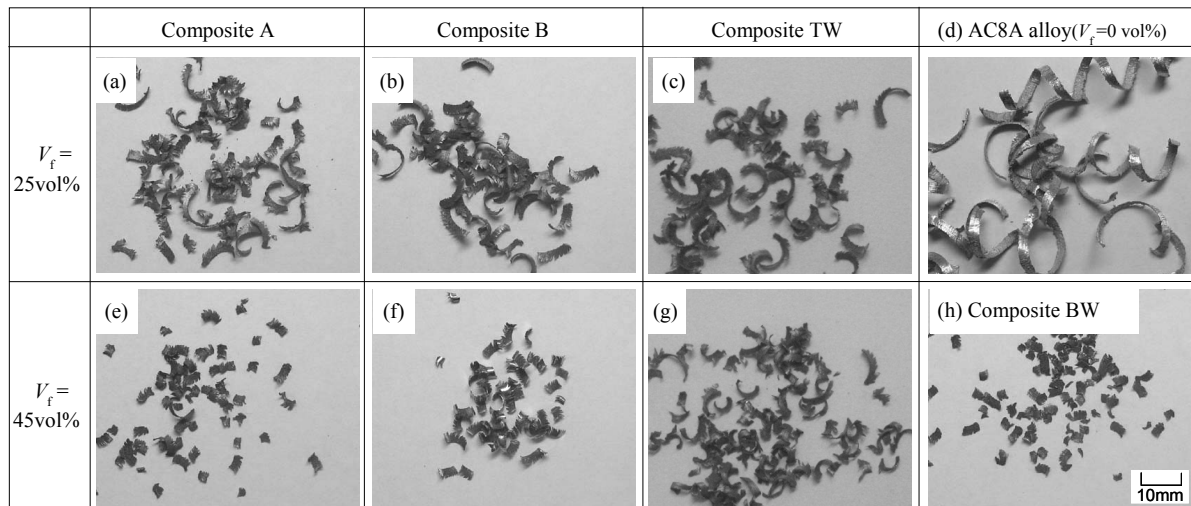


Figure 7. Chip forms of AC8A alloy and composites ($v = 100 \text{ m/min}$, $f = 0.1 \text{ mm/rev}$).

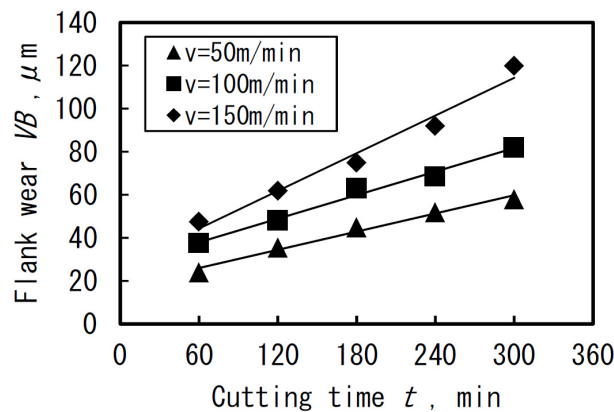


Figure 8. Effect of cutting time t on width of flank wear VB after cutting composite B ($V_f = 25 \text{ vol\%}$, $f = 0.1 \text{ mm/rev}$).

The width of the flank wear of the tool after cutting the AC8A alloy could not be measured because the tool edge was covered with the accretions. Figure 8 shows the effect of the cutting time t on the width of the flank wear (VB) after cutting composite B ($V_f = 25 \text{ vol\%}$, $f = 0.1 \text{ mm/rev}$). VB increases as v increases because the cutting distance increases along with v . Even if after cutting for 300 minutes at 150 m/min, however, VB was approximately 0.12 mm; this is lower than 0.2 mm, which is the tool life value for the finishing cut of nonferrous metals established in JIS. This result suggests that the composite can be machined for a long time without changing the tool. From the viewpoint of industrial applications, replacement of the carbide tool by the PCD tool would reduce the tool wear.

4 Conclusions

1. Reinforcement with the fibers or whiskers decreased the cutting force of the AC8A aluminum alloy. The cutting force of the short potassium titanate fiber-reinforced composite was lower than those of the whisker-reinforced composites.
2. The machined surfaces of the composites were smoother than that of the AC8A alloy. The machined surface and chip forms indicated that the fibers in the composite facilitated the shear deformation of the chips because the fibers were easily sheared by the cutting.
3. The fiber-reinforced composite can be consecutively machined for more than 300 minutes at 150 m/min without changing the carbide tool.

4. These results lead to the conclusion that the machinability of the composite is superior to that of the AC8A alloy.

References

- [1] Asano K. and Noguchi T. Trend of composite casting technology and joining technology for cast iron. *J.JFS*, **78**, pp. 96-105(2006).
- [2] Suganuma K. Interfacial microstructures of potassium titanate whiskers in pure aluminum and 6061 alloy matrix. *J. JAPAN Inst. METALS*, **58**, pp. 1213-1219(1994).
- [3] Harada H., Kudoh Y., Inoue Y. and Tsuchitori I. Preparation and mechanical properties of AC8A aluminum alloy composite reinforced with potassium titanate whisker. *J. JAPAN Inst. METALS*, **58**, pp. 69-77(1994).
- [4] Tsuchitori I. and Fukunaga H. Reactivity of potassium titanate whiskers with Al alloys. *J. JAPAN Inst. METALS*, **56**, pp. 333-341(1992).
- [5] Suganuma K., Fujita T. and Niihara K. Fabrication of aluminum matrix composite reinforced with potassium titanate whiskers by squeeze casting and microstructure of whiskers/matrix interface. *J. JAPAN Inst. METALS*, **54**, pp. 1422-1431(1990).
- [6] Nishida Y., Imai T., Yamada M., Matsubara H. and Shirayanagi I. Fabrication of potassium titanate whisker/aluminum composites and some their properties. *J.JILM*, **38**, pp. 515-521(1988).
- [7] Yamato H., Ohgami A., Akiyama I., Oyabu T., Morimoto Y., Ishimatsu S., Hori H., Higashi T. and Tanaka I. *Report of JAAST Meeting*, **16**, p.58(1994).
- [8] Kubota Co. *Data sheet for TXAX* (2005).
- [9] Asano K., Yoneda H. and Agari Y. Microstructure and thermal properties of short potassium titanate fiber/AC4A aluminum alloy composite fabricated by squeeze casting. *J.JFS*, **80**, pp. 8-14(2008).
- [10] Nishida Y. *Introduction to Metal Matrix Composites*, Corona Publishing, Tokyo (2001).
- [11] Saga T. and Ikeda S. Turning machinability of Al₂O₃-SiO₂ short-fiber reinforced ADC12 aluminum alloy composites. *J.JILM*, **41**, pp. 264-269 (1991).
- [12] Ed. by Kikai Kosakugaku Henshu Iinkai *Kikai Kosakugaku*, Sangyo Tosho, Tokyo (2003).
- [13] Yan B. and Wang C. Machinability of SiC particle reinforced aluminum alloy composite material. *J.JILM*, **43**, pp. 187-192(1993).